Nuclear Physics B (Proc. Suppl.) 4 (1988) 11–20
North-Holland, Amsterdam

GLUEBALL MASSES IN SU(3) LATTICE GAUGE THEORY

G. SCHIERHOLZ

Deutsches Elektronen-Synchrotron DESY
D-2000 Hamburg 52

and

Institut für Theoretische Physik der Universität Kiel
D-2300 Kiel

The use of local operators in lattice Monte Carlo glueball mass calculations has so far prevented a computation at small couplings and on large lattices. The reason is that their projection onto the low-lying glueball states decays rapidly into the statistical noise as the lattice spacing becomes smaller. To circumvent this problem one has to resort to nonlocal operators of lower dimensions. In this talk I shall construct such operators and present first results, so far for the 0^{++} and 2^{++} masses, of an ongoing effort to compute the glueball mass spectrum at small couplings and on large lattices.

1. INTRODUCTION

It is of fundamental importance to compute the glueball mass spectrum in the pure gauge theory on the lattice. On the one hand, QCD predicts the existence of glueballs, and a firm calculation of their masses would expose QCD to an invaluable quantitative test. There are indications that the inclusion of dynamical quarks does not change the masses of ordinary mesons and baryons significantly apart from a renormalization of the overall scale[1], and one may hope that the same would be true of the glueball masses. On the other hand, the calculation of the glueball mass spectrum in the quenched approximation is a necessary milestone which must be passed successfully before one can think of the realistic calculation.

First attempts to compute the glueball mass spectrum date from the early days of lattice gauge theory[2]. However, not until three years ago have calculations of the 0^{++} glueball mass been performed[3], which were reliable enough in their control of systematic and statistical errors as to address the question of finite size effects and the approach to the continuum limit. One of the results was that the 0^{++} glueball mass is subject to strong finite size corrections, and it was felt that one has to resort to larger lattices to progress. Furthermore, it turned out to be nearly impossible with the techniques of that time to extend the calculations beyond $\beta \equiv 6/g^2 = 5.9$, and attempts to compute the 2^{++} glueball mass failed completely.

If one cannot do an accurate calculation on large lattices, one may try to do it on small lattices. Indeed, a group of authors has computed the 2^{++} glueball mass on small spatial lattices. This was only possible by brute force using up to half a million of Monte Carlo sweeps each[4]. They found that the 0^{++} and the 2^{++} state have very similar masses. Recent analytic work by Koller and van Baal[5] has confirmed this result. But it also showed that rotational invariance is badly broken on small lattices, and that it is not restored until

$$z \equiv \frac{L}{\xi} \gg 5, \tag{1}$$

where L is the spatial extent of the lattice and ξ the correlation length. In addition, some of the mass ratios turned out to depend strongly on z in the region $z \lesssim 5$.

To shed further light on the credibility of the small volume calculations for continuum, infinite volume glueball masses, we have investigated the vacuum structure

0920–5632/88/$03.50

of $SU(2)$ gauge theory below and above $z = 5$. We found[6,7] that the topological susceptibility χ_t and the perimeter density of loops of color magnetic monopoles[8] l rise sharply at about $z = 5$ when going from small to large values of z. We interprete this result as evidence that the vacuum of the small volume is largely "perturbative", while only the large volume shows any sign of the nonperturbative dynamics like monopole condensation, which we believe is responsible for color confinement.

The conclusion to be drawn from all this is that the small volume calculations leave the glueball masses on large lattices largely undetermined.

From the calculation of various physical quantities we deduce furthermore that the scaling window for the Wilson action begins at $\beta = 6.0$. A meaningful glueball mass calculation therefore requires $\beta \geq 6.0$, and the volume should be large enough so that $z \gg 5$. In this talk I shall introduce a new method, which allows us to address glueball mass calculations in this region and report first results on 0^{++} and 2^{++} masses in $SU(3)$ gauge theory[9].

2. WHY DID EARLIER ATTEMPTS FAIL?

Before I shall present the new method, I want to explain the reason why our earlier attempts to compute the 0^{++} glueball mass on large lattices in the continuum region failed. Let $\Phi(t)$ be a color singlet, zero-momentum operator localized at time t with some spin, parity and charge conjugation quantum numbers. The lowest-lying glueball mass in that channel is then determined by computing the temporal decay of the correlation function

$$< 0|\Phi(t)\Phi(0)|\Omega >_c = \sum_{n=0}^{\infty} < 0|\Phi|n >< n|\Phi|\Omega > e^{-m_n t}$$

$$\stackrel{t \to 0}{=} c e^{-m_0 t}, \qquad (2)$$

where Ω stands for the vacuum ($\Omega = 0$) or a source ($\Omega = J$), and $m_0 \leq m_1 \leq m_2 \leq ... \leq m_\infty$. The subscript c denotes that the connected part is to be taken in case of the 0^{++} glueball. The success of the calculation will now depend on one's ability to construct operators that have a large projection onto the lowest-lying state. So far exclusively local operators, such as the $n \times m$ plaquette, have been used. Such operators have dimension $d = 4$. As a result one computes

$$c \propto a^5, \qquad (3)$$

where a is the lattice spacing. In practice this means that the projection onto the state whose mass one wants to calculate will rapidly drop and the signal be lost in the noise as the coupling constant is decreased. This was the reason why our earlier calculations[3] could not be extended beyond $\beta = 5.9$.

To confirm this statement, I have plotted the projection

$$p = \frac{c}{\sum_{n=0}^{\infty} < 0|\Phi|n >< n|\Phi|\Omega >} \qquad (4)$$

for various values of β in fig.1. This shows that the projection falls indeed like the fifth power of the lattice spacing, a^5, and that it is only of the order of a couple of percent at $\beta = 5.9$.

To overcome this problem one needs to construct operators of lower dimensions. Such operators exist. The price one has to pay is, however, that they are nonlocal. In the next section I shall discuss examples of such operators.

3. CHOICE OF OPERATORS

In the presence of a dynamical, scalar field φ an obvious choice for the 0^{++} operator would be $\Phi = \bar{\varphi}\varphi$, which has dimension $d = 2$. An analogous choice in the

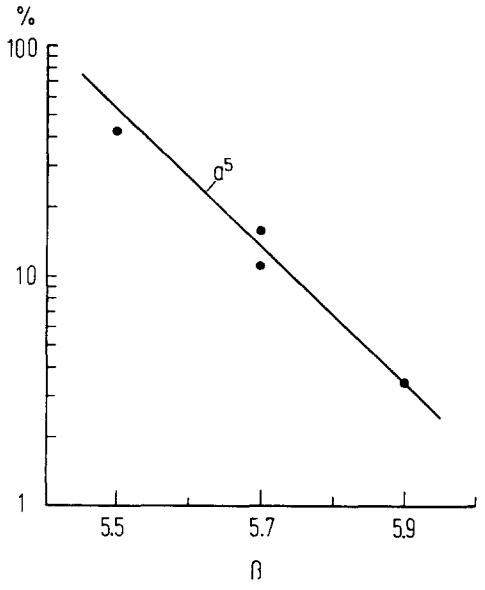

Figure 1: The projection p onto the lowest-lying 0^{++} glueball state as a function of β as computed in ref.3. The solid line represents the fifth power of the lattice spacing, a^5, renormalized to a constant string tension.

pure gauge theory is to take the inverse of the spatial, covariant Dirac operator,

$$\Phi(t) = tr(\not{d}(t) + m)^{-1}, \tag{5}$$

where

$$\not{d}(t) = \gamma_i(\partial_i + A_i)(t), \tag{6}$$

and this is the basic idea of the method.

We shall take staggered fermions, whose action is

$$S = \bar{\chi}(D + m)\chi,$$

$$\bar{\chi}D\chi = \sum_{n,\mu}(-1)^{\hat{x}_1+\ldots+\hat{x}_{\mu-1}}\hat{\chi}_n U_{n,\mu}\chi_{n+\hat{\mu}} - h.c., \tag{7}$$

where $n = (x_1, x_2, x_3, x_4 = t)$, and $\hat{\mu}$ is a displacement vector of one lattice unit in μ-direction. The particular type of fermions should, however, not matter. We then introduce Dirac operators

$$[d_i^{x_i}]_{(x_j,x_k),(x_j,x_k)+\hat{j}} =$$

$$(-1)^{\hat{x}_1+\ldots+\hat{x}_{j-1}}U_{(x_1,x_2,x_3,t),\hat{j}} - h.c.\,, \tag{8}$$

where $j, k \in \{1,2,3\}\backslash i$, $i \neq j$. They reside on spatial planes perpendicular to $\hat{i}$. From these we construct operators

$$\Phi_0(t) = \sum_{x_1} tr(d_1^{x_1}(t) + m)^{-1} + \sum_{x_2} tr(d_2^{x_2}(t) + m)^{-1}$$

$$+ \sum_{x_3} tr(d_3^{x_1}(t) + m)^{-1}, \tag{9}$$

and

$$\Phi_{2,1}(t) = \sum_{x_2} tr(d_2^{x_2}(t) + m)^{-1} - \sum_{x_3} tr(d_3^{x_3}(t) + m)^{-1},$$

$$\Phi_{2,2}(t) = \sum_{x_3} tr(d_3^{x_3}(t) + m)^{-1} - \sum_{x_1} tr(d_1^{x_1}(t) + m)^{-1},$$

$$\Phi_{2,3}(t) = \sum_{x_1} tr(d_1^{x_1}(t) + m)^{-1} - \sum_{x_2} tr(d_2^{x_2}(t) + m)^{-1}. \tag{10}$$

It is easily checked that Φ_0 ($\Phi_{2,m}$) projects onto the 0^{++} (2^{++}) glueball state and belongs to the representation A_1 (E). This is the simplest choice of operators of the kind (5), which allow to compute the 2^{++} mass at the same time as the 0^{++} mass. In forthcoming investigations we shall also employ proper 3-dimensional Dirac operators provided with the appropriate γ-matrices to compute the glueball masses of states of other parity and in different representations. It is obvious that L must be even for this choice of fermions.

The operators Φ_0 and $\Phi_{2,m}$ have dimension $d = 1$. For large times the correlation functions read

$$< 0|\Phi_0(t)\Phi_0(0)|0 >_c \overset{t\to\infty}{=} c_0 e^{-m_{0^{++}}t} \tag{11}$$

and

$$< 0|\Phi_{2,m}(t)\Phi_{2,m}(0)|0 >_c \stackrel{t\to\infty}{=} c_2 e^{-m_{2++}t}. \tag{12}$$

We now compute

$$c_{0,2} \propto a, \tag{13}$$

which is a clear improvement over (3).

4. NUMERICAL METHOD

The success of the numerical calculation will largely depend on the computer time needed to invert the Dirac operators. A fast algorithm to do so, which also needs relatively little storage, will be described below.

We write $d = iH$, where H is hermitean. The problem then is to compute $tr(iH + m)^{-1}$. In the first step we use the Lanczos algorithm[10] to tridiagonalize H:

$$X^{-1}HX = \begin{pmatrix} 0 & \beta_1 & 0 & \dots & 0 & 0 \\ \beta_1 & 0 & \beta_2 & \dots & 0 & 0 \\ 0 & \beta_2 & 0 & \dots & 0 & 0 \\ \vdots & \vdots & \vdots & \ddots & \vdots & \vdots \\ 0 & 0 & 0 & \dots & 0 & \beta_{N-1} \\ 0 & 0 & 0 & \dots & \beta_{N-1} & 0 \end{pmatrix}, \tag{14}$$

where X is unitary. This is done iteratively

$$\begin{aligned} \beta_1 x_2 &= H x_1, \\ \beta_i x_{i+1} &= H x_i - \beta_{i-1} x_{i-1},\ 2 \le i \le N-1, \\ \beta_n x_{N+1} &= H x_N - \beta_{N-1} x_{N-1}, \end{aligned} \tag{15}$$

where

$$X = (x_1, x_2, ..., x_N). \tag{16}$$

The starting vector x_1 is an arbitrary unit vector, which should be chosen such that rounding errors remain small. In case they build up and the column vectors x_i loose orthogonality, the latter have to be reorthogonalized from time to time with respect to the previous ones.

In the next step we compute the determinants of the tridiagonal matrices

$$M_n = \begin{pmatrix} m & i\beta_1 & \dots & 0 & 0 \\ i\beta_1 & m & \dots & 0 & 0 \\ \vdots & \vdots & \ddots & \vdots & \vdots \\ 0 & 0 & \dots & m & i\beta_n \\ 0 & 0 & \dots & i\beta_n & m \end{pmatrix}, \tag{17}$$

$$L_n = \begin{pmatrix} m & i\beta_{N-n+1} & \dots & 0 & 0 \\ i\beta_{N-n+1} & m & \dots & 0 & 0 \\ \vdots & \vdots & \ddots & \vdots & \vdots \\ 0 & 0 & \dots & m & i\beta_N \\ 0 & 0 & \dots & i\beta_N & m \end{pmatrix}, \tag{18}$$

which is done iteratively:

$$\begin{aligned} det(M_n) &= m det(M_{n-1}) + \beta_{n-1}^2 det(M_{n-2}), \\ det(L_n) &= m det(L_{n-1}) + \beta_{N-n+1}^2 det(L_{n-2}). \end{aligned} \tag{19}$$

Finally, we obtain

$$\begin{aligned} tr(iH + m)^{-1} = \frac{1}{det(M_N)} \{ & det(L_{N-1}) + \\ & det(M_1) det(L_{N-2}) + ... \\ & + det(M_{N-2}) det(L_1) + det(M_{N-1}) \}. \end{aligned} \tag{20}$$

All three steps are done in parallel for the various planes and/or masses. The time it takes to do all Dirac operator inversions turns out to be comparable to the time for 10 updates on the larger lattices. A more detailed description of the program can be found in ref. 4.

5. RESULTS

The idea is to compute the glueball masses for a range of spatial lattice sizes from the small to the very large and for several values of β. This will establish the lattice size needed for a meaningful glueball mass calculation. Furthermore, we expect that the transition from the "perturbative" to the nonperturbative vacuum at $z \approx 5$ will give us some clue about the mechanism of mass generation.

In our numerical calculations we choose antiperiodic boundary conditions for the fermions. The gauge fields are taken to be periodic and are simulated with the Wilson action using a standard Monte Carlo updating program[12].

The mass m is a free parameter, that may be tuned such as to maximize the projection onto the lowest-lying state or to minimize the error of the corresponding mass, which usually amounts to the same. The value of m, which gives the maximal projection, will give us some information about the size of the glueballs.

But m gives us also control over systematic errors. For large m only small loops contribute to Φ_0, $\Phi_{2,m}$, while for small m larger loops give the dominant contribution. So, for example, if our operators would couple to two states, one geometrically large and light and the other comparatively small and heavy, we would find a light mass for small m and a heavy mass for large m.

So far we have done simulations on the following sized lattices at the following values of β:

L^3T	β
$6^3 12$	5.7
$8^3 16$	5.85
$12^3 16$	5.85
$10^3 20$	6.0
$14^3 20$	6.0

Here T is the temporal extent of the lattice. The correlation functions are calculated for 20 mass values ranging from $m = 0.02$ to $m = 1.6$.

TEST OF THE METHOD

Before I shall present the results of the mass calculation, I want to demonstrate that the new method satisfies indeed our expectations. In figs. 2 and 3 I have plotted the correlation functions (11) and (12),

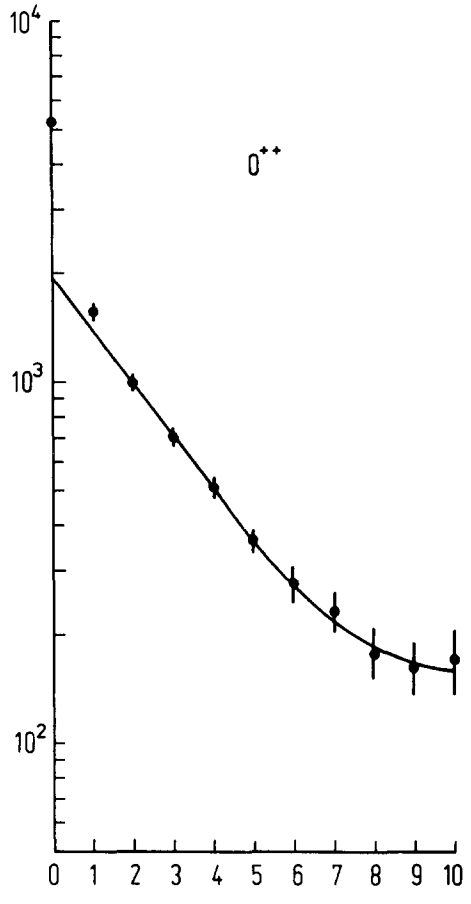

Figure 2: The 0^{++} correlation function on the $10^3 20$ lattice at $\beta = 6.0$ for $m = 0.1$ as a function of time. The solid line represents a single hyperbolic cosine fit.

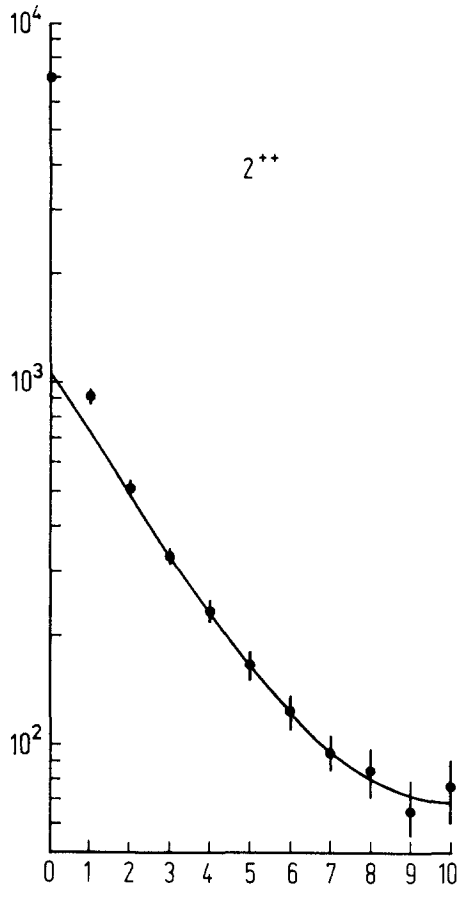

Figure 3: The 2^{++} correlation function on the $10^3 20$ lattice at $\beta = 6.0$ for $m = 0.1$ as a function of time. The solid line represents a single hyperbolic cosine fit.

respectively, on the $10^3 20$ lattice at $\beta = 6.0$. They are averaged over $\approx$ 20000 gauge field configurations. The striking result is that we obtain a clear signal now over the full temporal extent of the lattice, which accurately displays the asymptotic exponential decay. The projection onto the lowest-lying state has risen to $\approx 40\%$ for the 0^{++} and to $\approx 15\%$ for the 2^{++} glueball, which is not only large enough but also small enough not to hide any state of even smaller mass. We would certainly feel very uneasy if we had obtained a projection of $\approx 100\%$.

To verify the prediction (13) now, I have computed the projections

$$p_0 = \frac{c_0}{\sum_{n=0}^{\infty} |<0|\Phi_0|n>|^2} \tag{21}$$

and

$$p_2 = \frac{c_2}{\sum_{n=0}^{\infty} |<0|\Phi_{2,m}|n>|^2} \tag{22}$$

for the various values of β. The result is shown in fig. 4. The physical spatial volumes of the lattices have been chosen to be roughly equal. We find that both, p_0 and p_2, fall like a as we expect. This is to say that our method will also work at values of β larger than $\beta = 6.0$.

SYSTEMATIC ERRORS?

The projections p_0, p_2 depend, of course, on the mass parameter m. The numbers given in fig. 4 are their maximal values. For the lattices and β values we have investigated so far we find p_0, p_2 to assume their maxima for $m = 0.1 - 0.3$. I will give the precise values later. Outside this region p_0, p_2 drop significantly. Nevertheless, we are still able to compute the glueball masses rather accurately for $0.02 \leq m \leq 0.6$. In fig. 5 I have plotted the glueball masses $m_{0^{++}}a$ and $m_{2^{++}}a$ obtained on the $10^3 20$ lattice at $\beta = 6.0$ as a function of m. We find that both masses are independent of m within the statistical errors. (The procedure of fitting the Monte Carlo data will be described in the next paragraph.)

One might argue that the operators (9) and (10), because they are nonlocal and contain loops that go around the "world", couple to single quanta of electric flux. The result would be that the correlation functions (11) and (12) received an additional contribution with an effective mass KL, where K is the

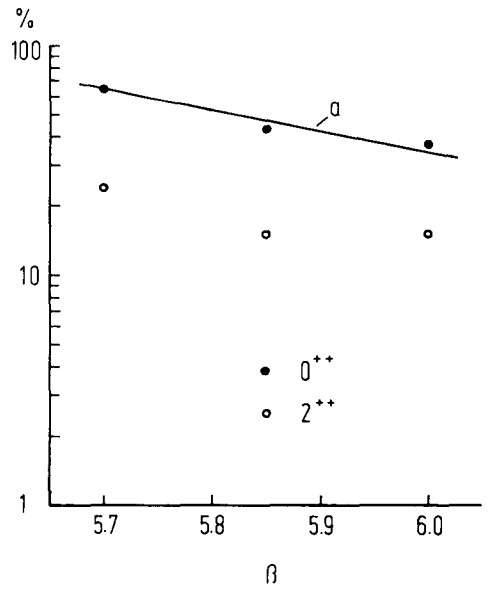

Figure 4: The projections p_0 and p_2 onto the lowest-lying 0^{++} and 2^{++} glueball states as a function of β on the $6^3 12$, $8^3 16$, $10^3 20$ lattices at $\beta = 5.7$, 5.85, 6.0, respectively. The solid line represents the lattice spacing, a, renormalized to a constant string tension.

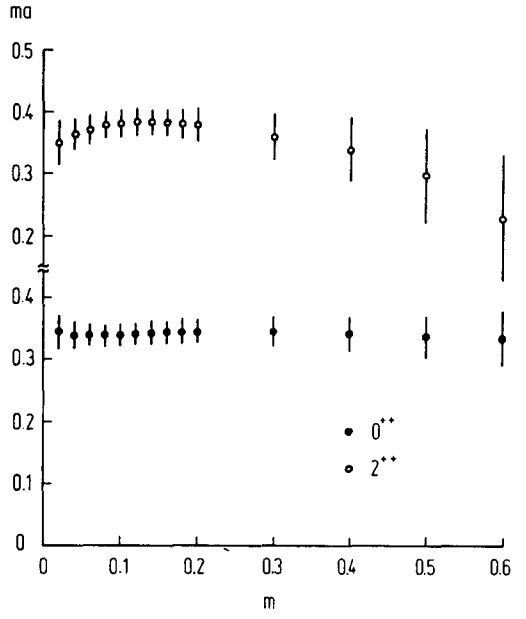

Figure 5: The glueball masses $m_{0^{++}}a$ and $m_{2^{++}}a$ on the $10^3 20$ lattice at $\beta = 6.0$ as a function of m.

string tension, which for small L could become dominant at large times. But this is not the case. For the sake of definiteness let us consider the 2^{++} state $|\Phi_{2,1} >= \int [dU] \Phi_{2,1} |U >$. Let us also restrict our discussion to $SU(2)$ for simplicity. It is easy to see now that $|\Phi_{2,1} >$ decomposes into four states, $|\Phi^{(l)}_{2,1} >$, $l = 1, ..., 4$. Each of these states belongs to the representation E, and they are classified according to their behavior under the global $Z(2)$ symmetry transformations $S^{(i)}$, which multiply each link in the x_i-direction at a given x_i-coordinate by -1. $|\Phi^{(1)}_{2,1} >$ is symmetric under all $S^{(i)}$, $|\Phi^{(2)}_{2,1} >$ is antisymmetric under $S^{(1)}$ and symmetric under $S^{(2)}$,$S^{(3)}$, $|\Phi^{(3)}_{2,1} >$ is symmetric under $S^{(1)}$ and antisymmetric under $S^{(2)}$,$S^{(3)}$ while $|\Phi^{(4)}_{2,1} >$ is antisymmetric under all $S^{(i)}$. It follows that the $|\Phi^{(l)}_{2,1} >' s$ are orthogonal to each other, and the lightest states they are coupling to are the 2^{++} glueball ($l = 1$), the 2^{++} glueball plus one quantum of electric flux in the x_1-direction ($l = 2$), two quanta of electric flux, one in the x_2 and the other in the x_3-direction, with opposite "charge" ($l = 3$) and three quanta of electric flux, respectively. Thus, the lowest competing mass is $2KL$, which on all our lattices is larger than $m_{2^{++}}$. Similar arguments apply for the 0^{++} state.

A further piece of information is the m-dependence of c_0, c_2. We find, e.g., on the $10^3 20$ lattice at $\beta = 6.0$:

$$c_0 \propto e^{-18m} \tag{23}$$

for $0.04 \leq m \leq 0.3$, while c_2 falls somewhat faster. This is close to what one would expect for the glueball wave function. For the expectation values of the "charged" operators one calculates, on the other hand, $< \Phi^{(l)} \Phi^{(l)} > \propto m^2$, $l \geq 2$. Hence, they are exponentially suppressed for small m.

0^{++} AND 2^{++} MASSES

To fit the correlation functions we discard the first two points and fit the remainder to a single hyperbolic cosine. The stability of the fit is checked by discarding further points. The errors are obtained by dividing the Monte Carlo data into sub-ensembles and taking the appropriate averages. Two such fits for the 0^{++} and 2^{++} correlation functions are shown in figs. 2 and 3.

The glueball masses that we have obtained hitherto are listed in the table below:

β	L^3T	$m_{0^{++}}a$	$m_{2^{++}}a$
5.7	$6^3 12$	0.74 ± 0.04	0.73 ± 0.03
5.85	$8^3 16$	0.54 ± 0.04	0.50 ± 0.04
6.0	$10^3 20$	0.34 ± 0.02	0.38 ± 0.02
6.0	$14^3 20$	0.63 ± 0.08	0.97 ± 0.15

(24)

The result on the $14^3 20$ lattice should be regarded as preliminary, as we have accumulated only ≈ 8000 gauge field configurations yet in this case.

Where our results overlap with previous calculations, that is on the $6^3 12$ lattice with ref. 3 and on the $14^3 20$ lattice with ref. 13 in case of the 0^{++} mass, we find general agreement within the errors. At this conference Marinari[14] and Michael[15] have also reported new results on 0^{++} and 2^{++} glueball masses, which are consistent with this and our old work[3].

The mass parameter m, which gives the largest projection, comes out to be $m = 0.3$ on the $6^3 12$ lattice and $m = 0.1$ on the $8^3 16$ lattice for both states, while on the $10^3 20$ lattice we find $m = 0.1$ for the 0^{++} and $m = 0.12$ for the 2^{++}, and on the $14^3 20$ lattice $m = 0.12$ for the 0^{++} and $m = 0.14$ for the 2^{++} state.

DISCUSSION

The glueball masses (24) fall into two regions, one with $z \approx 4$ and the other with $z \approx 9$. The main new result of our work is that the masses and mass ratios are rather distinct in the two regions, which, after what I have said in the introduction, comes not really as a surprise. I will discuss this now in some detail.

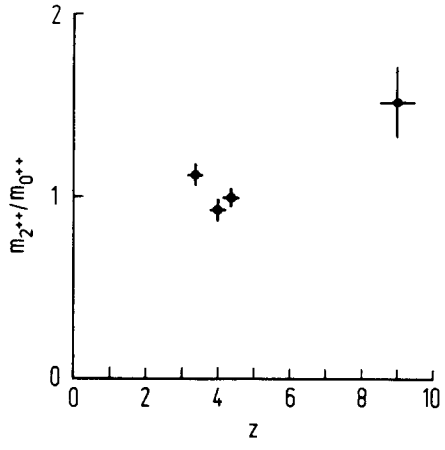

Figure 6: The mass ratio $m_{2^{++}}/m_{0^{++}}$ as a function of z.

Let us first consider the 2^{++} to 0^{++} glueball mass ratio, which has been the matter of heated debate during the last year. In fig. 6 I have plotted $m_{2^{++}}/m_{0^{++}}$ as a function of z. We find that the ratio rises from ≈ 1 at $z \approx 4$ to ≈ 1.5 at $z \approx 9$. This rise cannot be explained by ordinary (large volume) finite size effects[16] but indicates a transition in the vacuum structure. At present we do not understand precisely the nature of this transition. There are indications in $SU(2)$ gauge theory that color magnetic monopoles condense[8*] for $z \geq 5$ and (consequently?) that the ground state energy becomes negative[5] at $z \approx 5$. This would mean

*The calculations in ref. 8 were done on the symmetric, 5^4 lattice as well as on the asymmetric, $10^3 5$ lattice. Both gave the same results, so that we showed only the results on the larger, asymmetric lattice. Because of the small spatial volume associated with the transition we can, however, not speak of a phase transition here.

that confinement sets in dynamically only at $z \approx 5$. It would be very interesting now to do a *simultaneous* calculation of the glueball masses and, e.g., the perimeter density of monopole loops[7,8] l for several values of z, in particular near $z = 5$.

At the small values of z the ratio agrees with the small volume calculations in refs. 4 and 5. From the mass m, which maximizes the projection onto the lowest-lying state, we judge that the 2^{++} glueball is geometrically only slightly smaller than the 0^{++} glueball.

The 0^{++} mass itself does also increase as z increases. To exhibit this I have plotted the ratio $m_{0^{++}}/\sqrt{K}$ as a function of z in fig 7. Also shown is the ratio $m_{2^{++}}/\sqrt{K}$. The string tension is taken from ref. 17 and, when necessary, interpolated. Its lattice size dependence is assumed to be given by

$$K(L) = K(\infty) - \frac{\pi}{3L}, \tag{25}$$

which is supported by Monte Carlo calculations. I have also included our previous[3] 0^{++} masses in the plot. The observation that the vacuum becomes unstable under the condensation of color magnetic monopoles at $z \approx 5$, which is followed by a lowering of the ground state energy, could also explain this sudden increase.

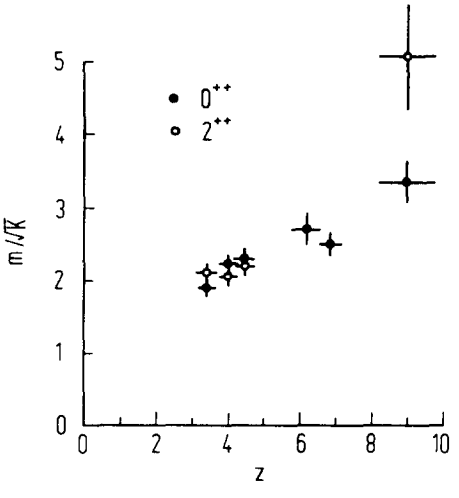

Figure 7: The ratios $m_{0^{++}}/\sqrt{K}$ and $m_{2^{++}}/\sqrt{K}$ as a function of z.

Figure 7 indicates also that the ratio $m_{0^{++}}/\sqrt{K}$ is a remarkably universal function of z. It does, however, not allow any conclusions yet as to what the asymptotic values of the 0^{++} and, even less, the 2^{++} glueball masses are.

6. CONCLUSIONS

This work is certainly only a first step towards the calculation of continuum glueball masses. It shows clearly how important it is to gain control over finite size effects. In the future we will have to do accurate calculations on still larger lattices until the mass ratios and the ratios $m_{0^{++}}/\sqrt{K}$, $m_{2^{++}}/\sqrt{K}$ show a plateau in z, and all that must be repeated at larger values of β. This will require an order of magnitude more computer time. But it is feasible now, and we are going to do it.

ACKNOWLEDGEMENTS

This work summarizes work I have done in collaboration with Andreas Kronfeld and Kevin Moriarty. It is a pleasure to thank both of them for their efforts in making this project succeed. Furthermore, I am indebted to J. Speth for granting me computer time on the CRAY-XMP at the KFA in Jülich, where the ideas behind this work were tested first, and the John von Neumann National Supercomputer Center and the Control Data Corporation for access to their CYBER 205's, on which the results presented here were obtained. Last not least, I like to thank M. Lüscher for useful conversations.

REFERENCES

1. M. Fukugita, this conference
2. M. Falcioni, E. Marinari, M. L. Paciello, G. Parisi, F. Rapuano, B. Taglienti and Zhang Yi-cheng, Phys. Lett. 110B, 295 (1982);

K. Ishikawa, G. Schierholz and M. Teper, Phys. Lett. 110B, 399 (1982);
B. Berg, A. Billoire and C. Rebbi, Ann. Phys. 142, 185 (1982)

3. Ph. de Forcrand, G. Schierholz, H. Schneider and M. Teper, Phys. Lett. 152B, 107 (1985)

4. B. Berg, A. Billoire and C. Vohwinkel, Phys. Rev. Lett. 57, 400 (1986)

5. P. van Baal, Stony Brook preprint ITP-SB-86-79 (1986), to appear in the proceedings of *Lattice Gauge Theory 1986*;
J. Koller and P. van Baal, Phys. Rev. Lett. 58, 2511 (1987);
J. Koller and P. van Baal, Stony Brook preprint ITP-SB-87-47 (1987)

6. M. Kremer, A. S. Kronfeld, M. L. Laursen, G. Schierholz, C. Schleiermacher and U.-J. Wiese, in preparation

7. A. S. Kronfeld, M. L. Laursen, G. Schierholz and U.-J. Wiese, DESY preprint 87-073 (1987), to be published in Phys. Lett. B

8. A. S. Kronfeld, G. Schierholz and U.-J. Wiese, Nucl. Phys. B293, 461 (1987)

9. A. S. Kronfeld, K. J. M. Moriarty and G. Schierholz, in preparation

10. I. M. Barbour, N.-E. Behilil, P. E. Gibbs, G. Schierholz and M. Teper, in *The Recursion Method and its Applications*, eds. D. G. Pettifor and D. L. Weaire, Springer Series in Solid State Sciences 58 (Springer, Berlin, Heidelberg, New York, Tokyo, 1985)

11. A. S. Kronfeld, K. J. M. Moriarty and G. Schierholz, Princeton preprint JVNC-87-1 (1987), submitted to Comput. Phys. Comm.

12. M. Campostrini, K. J. M. Moriarty and C. Rebbi, Comput. Phys. Comm. 42, 175 (1986)

13. T. A. DeGrand, Phys. Rev. D36, 176 (1987)

14. E. Marinari, this conference

15. C. Michael, this conference

16. M. Lüscher, Comm. Math. Phys. 104, 177 (1986)

17. Ph. de Forcrand, G. Schierholz, H. Schneider and M. Teper, Phys. Lett. 160B, 137 (1985)